CrystEngComm

Accepted Manuscript

ROYAL SOCIETY OF CHEMISTRY

www.rsc.org/crystengcomm

Journal Name

RSCPublishing

COMMUNICATION

Predicting and creating 7-connected Zn_4O vertices for the construction of exceptional metal-organic framework with nanoscale cages

Shizhe Bai, Weiquan Zhang, Yun Ling, Feilong Yang, Mingli Deng,* Zhenxia Chen, Linhong Weng, and Yaming Zhou*

Cite this: DOI: 10.1039/x0xx00000x

Received 00th January 2012,
Accepted 00th January 2012

DOI: 10.1039/x0xx00000x

www.rsc.org/

A 7-connected Zn_4O unit has been theoretically predicted based on the model of basic zinc acetate $[Zn_4O(CH_3COO)_6]$, which was then experimentally extended into three-dimensional structure featuring three kinds of nanocages in a unit cell.

Crystal engineering of metal-organic frameworks (MOFs, or porous coordination polymers, PCPs) has been the subject aimed at creating novel crystalline porous materials with intriguing artificial architectures [1, 2] and/or functionalities for potential applications. [3-10] During the past decades, it has been witnessed that the reticular synthesis strategy based on secondary building units (SBUs) have greatly led to the proliferation of MOFs. It now comes to realize that SBUs are essential to the design of directionality for the construction of MOFs since they serve as the organizing concept for the classification of structures into their underlying topologies. [11, 12] Taking the 6-connected $[Zn_4O(O_2C)_6]$ (Zn_4O-6) SBU for an example, [13] it has been extended to numerous porous structures including 6-connected *pcu* net, (3,6)-connected *ttu* or *act* net, [14-15] (4,6)-connected *cor* net. [16]

It is expected that the continued incremental increases of MOFs can be achieved by the strategy of using these well-defined SBUs with different organic struts. [17, 18] However, the kinds of frameworks may ultimately meet limitations, since the organic struts have limited geometries to extend the SBUs (nodes) into more nets. In addition, the SBUs with extending degree in even numbers are commonly observed among the reported structures, whereas even-connected nodes, in some cases, are preferred to form interpenetrated nets (such as *pcu*, *dia*) when longer linkers are used, consequently leading to low degrees of porosity. [19, 20]

An alternative strategy to achieving novel frameworks meanwhile avoiding the interpenetration in MOFs is to address SBUs. Several groups have shown a way by expanding the sizes of SBUs. [21-25] Here, in this paper, we introduce another way for the construction of novel frameworks by tuning the extending degree of a well-defined SBU. This idea is borrowed from the phenomenon of the ligand addition reaction of a mononuclear complex. With the additional ligand coordinates to the metal center, the coordination geometry will change with the process, leading to the formation of a new structure. Considering the SBUs for MOF structures, if a pair of metal ions in a SBU changes their coordination numbers synchronously by addition reaction of a bridging ligand, it will leads the changes of the extending degree of a certain SBU. With this in mind, an energy stable 7-connected $[Zn_4O(CH_3COO)_7]^-$ SBU (Zn_4O-7) was predicted by theoretical simulation of the reaction from the classic basic zinc acetate $[Zn_4O(CH_3COO)_6]$ (Zn_4O-6) with additional acetate ligand. Then we experimentally demonstrate how the predicted 7-connected vertices be assembled into a MOF structure, $\{[(Zn_4O)_2(H_2O)_2(bptc)_{3.5}]\cdot 2CH_3NH_3\cdot xG\}_n$ (**1**, H_4bptc = [1,1'-biphenyl]-3,3',5,5'-tetracarboxylic acid, CH_3NH_3 = protonated methanamine, G = guest water molecules) , which features a novel (4,7)-connected net with a symbol point of $(4^4.6^2)_4(4^{10}.6^{11})_2$ and contains three kinds of cages with sizes range from micro to meso scales.

To vary the extending degree of a certain SBU, the existence of metal ion with variable coordination number is prerequisite. In the case of Zn_4O-6, each Zn ion is in four-coordinated tetrahedral geometry. Previous reports have shown that the coordination numbers of Zn ions in this prototype SBU were variable, for examples: 6-connected Zn_4O-6 SBU with one of the Zn(II) ions in six-coordinated octahedral geometry, [26] 12-connected $[Zn_4O(CO_2)_6]_2\cdot H_2O$ SBU built of two Zn_4O SBU with a μ-H_2O through two Zn(II) ions in trigonal bipyramidal geometries, [27] and 10/12-connected Zn_7O_2 SBU based on two Zn_4O SBUs by sharing one Zn(II) in six coordinated octahedral geometry. [28]

Taking the previous reports in consideration, a simulated model based on optimized structure of basic zinc acetate (Zn_4O-6) with addition of η_1-CH_3COO^- ligand was built (Fig S1 and Table S1). Geometries of predicted reactants, products, and transition states for the ligand addition reaction in this model are shown in Fig. 1. The CH_3COO^- in the reactant model tends to have carbonyl group directed at the electron hole of Zn_4O-6 SBU, and gradually changed from η_1 to $\mu_{1,2}$-coordination model by binding on another metal ion (Fig.1d, e, f). This process is different from the ligand displacement reaction of Zn_4O-

6 induced by water molecule,[29] where the water molecule ends up one of $\mu_{1,2}$-carboxylate with its oxygen bonded to the metal and its proton pointing at the displaced oxygen atom of the carboxylate. Here, the ligand addition reaction of Zn_4O-6 happens because of the strong electro donor-acceptor interaction between carbonyl and Zn(II). The calculated results demonstrate the

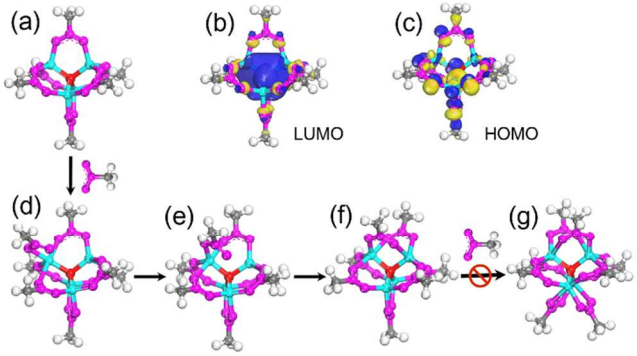

Fig. 1. (a) geometry optimized structure of basic zinc acetate; (b) and (c) the frontier molecular orbital profiles; (d) and (e) the snap structures of transition states of the ligand addition reaction; (f) and (g) the geometry optimized product of $[Zn_4O(CH_3COO)_7]^-$ and $[Zn_4O(CH_3COO)_8]^{2-}$.

generation process of the Zn_4O-7 SBU is exothermic (Table 1). Moreover, the Gibbs free energy for this reaction shows that the formation of the Zn_4O-7 SBU is spontaneous because of the negative value. While further ligand addition reaction leads to Zn_4O-8 seems not favourable because of the positive value (Table S2 and S3). It should be mentioned that the predicted Zn_4O-8 is different from the previously reported one, in which there are only four carboxylate groups in $\mu_{1,2}$-bridge model. [30] The results indicate that creating Zn_4O-7 is favourable for the construction of novel MOF structures.

Table 1. The theoretically calculated enthalpy and Gibbs free energy of the ligand addition reaction.

	ΔG (kcal/mol) [a]		*ΔH* (kcal/mol) [a]	
	Zn_4O-7	Zn_4O-8	Zn_4O-7	Zn_4O-8
PW91	-31.275	5.708	-43.673	-18.448
BP	-23.755	28.183	-37.804	-1.100
PBE	-33.193	6.215	-42.367	-15.878
BLYP	-28.931	/ [b]	-35.969	/ [b]

[a] $Zn_4O(CH_3COO)_6 + n\ CH_3COO \rightarrow [Zn_4O(CH_3COO)_{6+n}]^{n-}$, $n = 1$ for Zn_4O-7 and $n = 2$ for Zn_4O-8.
[b] The energy didn't converge in 100 SCF steps

Based on the simulation results, the experimental construction of Zn_4O-7 in MOFs were carried out by using bptc as the ligand. After careful screening the synthetic conditions (Table S4), colourless bulk crystal samples of **1** were finally obtained by solvothermal reaction of $Zn(OAc)_2$ and H_4bptc in the solution of DMF and HNO_3 at 140 °C for three days (ESI †). Pure crystal phase of bulk samples was confirmed by X-ray powder diffraction (Fig. S2). Single-crystal X-ray diffraction analysis reveals that **1** crystallizes in the cubic system *I3-a* space group with the cell parameter of $a = b = c = 52.62$ Å (Table S5), which is built of $Zn_4O(COO)_7$ (SBU-I), $Zn_4O(COO)_7(H_2O)_2$ (SBU-II) together with bptc ligands (Fig. 2a-c). Both of these two SBUs have the same extending geometry as the theoretical prediction. The difference between SBU-I and SBU-II stems from the coordination geometries of the paired Zn(II) ions. In SBU-I, Zn(1) and Zn(2) locate in five-coordinated trigonal bipyramidal geometries, while Zn(5) and Zn(6) are in six-coordinated distorted octahedral geometries in SBU-II because of coordinated water molecules (Fig. S3, Table S6 for detailed bond distances). Since the 1-negative charge of Zn_4O-7, the framework has a net 2-negative charge per formula unit. Two methylammonium cations (products of DMF decomposition) per formula unit reside in the pores to balance the charge as evidenced by single crystal and elemental analysis data.

A prominent structural feature of **1** is the presence of three kinds of

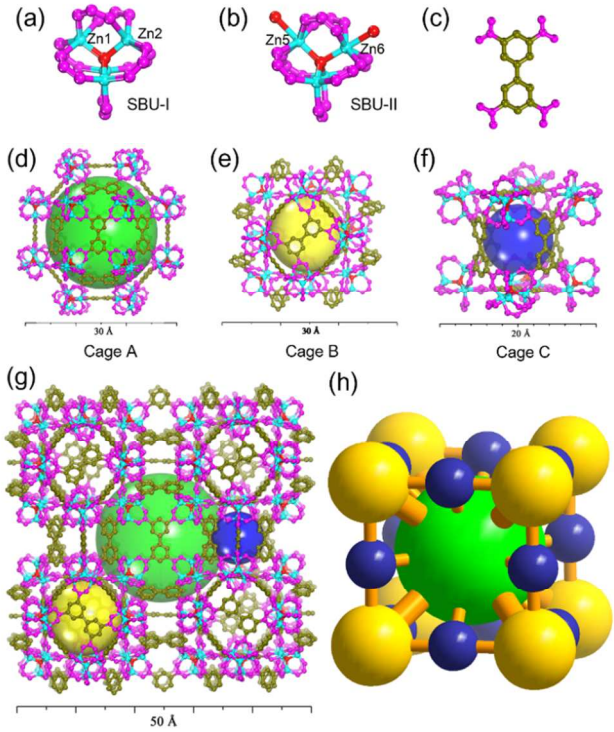

Fig.2. Structural motif of SBU-I (a) and SBU-II (b) and the bptc ligand (c); (d)-(f) the three kinds of cage structures formed by Zn_4O-7 and bptc ligand; (g) three-dimensional structure of 1; (f) the cage structures of 1. (green, yellow and blue balls shows the cage A, cage B and cage C respectively)

cages with sizes range from micro to meso scales (Fig. 2d-f). Cage A, the largest one (Fig. 2d), is made up of 24 Zn_4O-7 SBUs and 18 bptc ligands; the overall edge length is about 27 Å and the inner diameter based on the van der Waals surfaces is about 23 Å. Cage B (Fig. 2e) consists of 12 Zn_4O-7 SBUs and 8 bptc ligands; the size of cage B is about 16 Å with the inner diameter of about 12 Å. The smallest cage C (Fig. 2f) contains 8 Zn_4O-7 SBUs and 8 bptc ligands, of which the size is about 12 Å with the inner diameter of about 8 Å. Finally, in a unit cell, each cage A is connected to 6 adjacent cage A, 8 cage B and 12 cage C by sharing windows. The window sizes are of ~2.8 and ~ 4.6 Å, which are filled by guest water molecules and methylammonium cations respectively (Fig. S4). After theoretically removing the guests, the solvent accessible volume per unit cell is ca. 65 % and the surface areas is ca. 881 m^2/g (Fig. S5). Such kind of structure consisting of three kinds of cages was rarely observed in node-type MOFs.

Further insight into this framework is carried out by topological analysis. As predicted by the simulation, the SBU-I and SBU-II can be considered as 7-connected nodes (Fig. S6). The bptc ligand, is firstly regarded as a 3-connected node with one direction connected itself. Therefore, the framework of **1** can be regarded as a (3,3,7)-connected net. Topological analysis revealed a complex short (Schläfli) vertex symbol. Then, the two 3-connected nodes of a bptc ligand is fused into a 4-connected node, the framework of **1** thereby transforms into a (4,7)-connected net with the short (Schläfli) vertex symbol of $(4^4.6^2)_4{\cdot}(4^{10}.6^{11})_2$ (Fig. 3). The topology analyses for both (3,3,7) or (4,7)-connected net confirms that they are totally novel networks without interpenetration, which could be ascribed to the unprecedented odd-connected Zn_4O-7 SBUs.

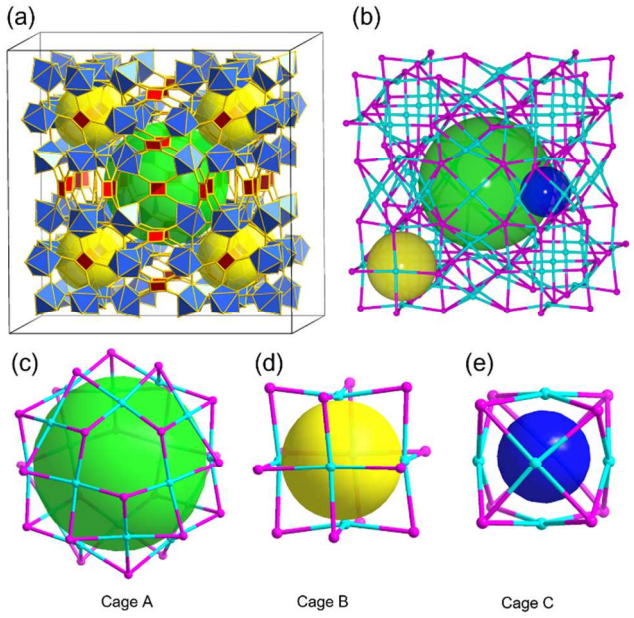

Fig.3. (a) Considering the abstraction of the Zn_4O-7 SBU as a distorted pentagonal bipyramid and the ligand as a square of **1**; (d) a (4, 7)-connected net of **1** after reducing the vertices into nodes; (c)-(e) the cage structures of A, B, C given in the node-type forms.

We then assessed the thermal and air stability of **1** (Fig. S7). A weight loss of 16.1 % in the range of 30 ~ 170 °C is observed, which could be ascribed to the loss of guest molecules. Then there is no obvious weight loss until to 360 °C, where a 28.1 % weight loss is followed, indicating the thermolysis of **1** under N_2 flow. The air stability of **1** was studied in air condition after being exposed for 8 h (Fig. S8). The PXRD pattern shows that the diffraction peak at $2\theta = 3.4^o$ is completely disappeared, indicating the phase transformation of **1** due to the loss of guest solvents. [31] The results indicate that the thermal and air stability of **1** is similar to that MOFs built of Zn_4O-6 SBUs. [32-34]

Gas sorption using N_2 or Ar as probe molecule was then carried out, while no detective BET data were obtained. It can be explained that (i) the small window sizes may block the diffusion of probe molecules; (ii) the guest molecules are hardly be removed because methylammonium cations balance the charges of the framework; (iii) the loss of guest molecules may cause the damage of the framework. [35] The photoluminescent spectra of as-made **1** (Fig. S9) and the free ligand H_4bptc in solid states were then measured at room temperature. **1** shows a blue emission spectra with a peak at 443 nm upon excitation at 349 nm, whereas the free ligand exhibits a purple emission with a peak at 366 nm when it was excited by 317 nm. The observable red-shift of the emission spectra can be ascribed to the ligand-to-metal charge-transfer (LMCT) effect in **1**. [36-39]

In summary, we report the theoretical prediction of a novel metal-carboxylate cluster ($Zn_4O(CH_3COO)_7^-$, Zn_4O-7) based on the model of basic zinc acetate ($Zn_4O(CH_3COO)_6$). Extending this odd-connected Zn_4O-7 vertices by a simple tetrcarboxylate linker, a novel MOF structure containing three kinds of nanocages in a unit cell has been experimentally isolated, which features a novel (4,7)-connected net with a symbol point of $(4^4.6^2)_4(4^{10}.6^{11})_2$. Our result shows another feasible way to create new kind of MOF structures by varying the extending degree of well-defined SBUs based on theoretical prediction.

Acknowledgements

We gratefully acknowledge the financial support from NSFC (No. 21203032, 21101031), the Shanghai Leading Academic Discipline Project (B108), the Program for Changjiang Scholars and Innovative Research Team in University (IRT1117).

Notes and references

Shanghai Key Laboratory of Molecular Catalysis and Innovative Materials, Department of Chemistry, Fudan University, Shanghai, 200433, China.
E-mail: mldeng@fudan.edu.cn; ymzhou@fudan.edu.cn; Fax: +86 21 65643925; Tel: +86 21 65642261.
Electronic Supplementary Information (ESI †) available: [Synthesis, crystal data, energy and theoretical BET surface area calculation results, PXRD, TGA data, PL spectra, etc]. See DOI: 10.1039/c000000x/

1 M. O'Keeffe and O. M. Yaghi, *Chem. Rev.*, 2012, **112**, 675−702.
2 J. J. Perry IV, P. L. Feng, S. T. Meek, K. Leong, F. P. Doty and M. D. Allendorf, *J. Mater. Chem.*, 2012, **22**, 10235−10248.
3 K. Sumida, D. L. Rogow, J. A. Mason, T. M. McDonald, E. D. Bloch, Z. R. Herm, T.H. Bae and J. R. Long, *Chem. Rev.*, 2012, **112**, 724−781.
4 Y. J. Cui, Y. F. Yue, G. D. Qian and B. L. Chen, *Chem. Rev.*, 2012, **112**, 1126−1162.
5 H. Wu, Q. Gong, D. H. Olson and J. Li, *Chem. Rev.*, 2012, **112**, 836−868.
6 L. E. Kreno, K. Leong, O. K. Farha, M. Allendorf, R. P. Van Duyne and J. T. Hupp, C *Chem. Rev.*, 2012, **112**, 1105−1125.
7 P. Horcajada, R. Gref, T. Baati, P. K. Allan, G. Maurin, P. Couvreur, G. Ferey, R. E. Morris and C. Serre, *Chem. Rev.*, 2012, **112**, 1232−1268.
8 J. R. Li, R. J. Kuppler and H. C. Zhou, *Chem. Soc. Rev.*, 2009, **38**, 1477−1504.
9 L. J. Murray, M. Dinca and J. R. Long, *Chem. Soc. Rev.*, 2009, **38**, 1294−1314.
10 M. Kurmoo, *Chem. Soc. Rev.*, 2009, **38**, 1353−1379.
11 D. J. Tranchemontagne, J. L. Mendoza-Cortes, M. O'Keeffe and O. M. Yaghi, *Chem. Soc. Rev.*, 2009, **38**, 1257−1283.

12 M. Li, D. Li, M. O'Keeffe and O. M. Yaghi, *Chem. Rev.*, 2014, **114**, 1343−1370.
13 H. Li, M. Eddaoudi, M. O'Keeffe and O. M. Yaghi, *Nature*, 1999, **402**, 276−279.
14 R. Grünker, I. Senkovska, R. Biedermann, N. Klein, M. R. Lohe, P. Müller and S. Kaskel, *Chem. Commun.*, 2011, **47**, 490−492.
15 D. Sun, D. J. Collins, Y. Ke, J.L. Zuo and H.C. Zhou, *Chem. Eur. J.*, 2006, **12**, 3768−3776.
16 Z. X. Chen, S. C. Xiang, T. B. Liao, Y. T. Yang, Y. S. Chen, Y. M. Zhou, D. Y. Zhao, B. L. Chen, *Cryst. Growth Des.*, 2010, **10**, 2775−2779.
17 M. Eddaoudi, J. Kim, N. Rosi, D. Vodak, J. Wachter, M. O'Keeffe and O.M. Yaghi, *Science* 2002, **295**, 469−472.
18 H. X. Deng, C. J. Doonan, H. Furukawa, R. B. Ferreira, J. Towne, C. B. Knobler, B. Wang and O. M. Yaghi, *Science*, 2010, **327**, 846−850.
19 T. M. Reineke, M. Eddaoudi, D. Moler, M. O'Keeffe and O. M. Yaghi, *J. Am. Chem. Soc.*, 2000, **122**, 4843−4844.
20 S. K. Elsaidi, M. H. Mohamed, L. Wojtas, A. Chanthapally, T. Pham, B. Space, J. J. Vittal and M. J. Zaworotko, *J. Am. Chem. Soc.*, 2014, **136**, 5072−5077.
21 J. An, O. K. Farha, J. T. Hupp, E. Pohl, J. I. Yeh and N. L. Rosi, *Nat. Commun.*, 2012, **3**, 604.
22 J. R. Li, J. M. Yu, W. G. Lu, L. B. Sun, J. L. Sculley, P. B. Balbuena and H. C. Zhou, *Nat. Commun.*, 2013, **4**, 1538.
23 J. H. Cavka, S. Jakobsen, U. Olsbye, N. Guillou, C. Lamberti, S. Bordiga, and K. P. Lillerud, *J. Am. Chem. Soc.*, 2008, **130**, 13850–13851.
24 A. Dolbecq, C. Mellot-Draznieks, P. Mialane, J. Marrot, G. Férey and F. Sécheresse, *Eur. J. Inorg. Chem.*, 2005, **15**, 3009–3018.
25 D. T. Vodak, M. E. Braun, J. Kim, M. Eddaoudi and O. M. Yaghi, *Chem. Commun.*, 2001, **24**, 2534–2535.
26 C. D. Madhab, H. Xu, Z. Y. Wang, G. Srinivas, Wei Zhou, Y. F. Yue, V. N. Nesterov, G. D. Qian and B. L. Chen, *Chem. Commun*., 2011, **47**, 11715−11717.
27 P. Shen, W. W. He, D. Y. Du, H. L. Jiang, S. L. Li, Z. L. Lang, Z. M. Su, Q. Fu and Y. Q. Lan, *Chem. Sci.*, 2014, **5**, 1368–1374.
28 Q. S. Zheng, F. L. Yang, M. L. Deng, Y. Ling, X. F. Liu, Z. X. Chen, Y. H. Wang, L. H. Weng and Y. M. Zhou, *Inorg. Chem.*, 2013, **52**, 10368–10374.
29 J. J. Low, A. I. Benin, P. Jakubczak, J. F. Abrahamian, S. A. Faheem and R. R. Willis. *J. Am. Chem. Soc.*, 2009, **131**, 15834–15842.
30 A. Burgun, R. S. Crees, M. L. Cole, C. J. Doonana and C. J. Sumby, *Chem. Commun*., 2014, **50**, 11760−11763.
31 C. P. Li and M. Du, *Chem. Commun*., 2011, **47**, 5958−5972.
32 H. Furukawa, N. Ko, Y. B. Go, N. Aratani, S. B. Choi, E. Choi, A. O. Yazaydin, R. Q. Snurr, M. O'Keeffe, J. Kim and O. M. Yaghi, *Science*, 2010, **239**, 424−428.
33 K. Koh, A. G. Wong-Foy and A. J. Matzger, *J. Am. Chem. Soc.*, 2009, **131**, 4184−4185.
34 J. L. C. Rowsell, E. C. Spencer, J. Eckert, J. A. K. Howard and O. M. Yaghi, *Science,* 2005, **309**, 1350−1354.
35 M. Du, M. Chen, X. Wang, J. Wen, X. G. Yang, S. M. Fang and C. S. Liu, *Inorg. Chem.*, 2014, **53**, 7074–7076.
36 S. S. Kaye, A. Dailly, O. M. Yaghi and J. R. Long, *J. Am. Chem. Soc.*, 2007, **129**, 14176−14177.
37 Z. Lin, L. Chen, C Yue, C. Yan, F. Jiang and M. Hong, *Inorg. Chim. Acta*., 2008, **361**, 2821−2827.
38 D. F. Sava, L. E. S. Rohwer, M. A. Rodriguez and T. M. Nenoff, *J. Am. Chem. Soc.*, 2012, **134**, 3983−3986.
39 F. L. Yang, Q. S. Zheng, Z. X. Chen, Y. Ling, X. F. Liu, L. H. Weng and Y. M. Zhou, *CrystEngComm*., 2013, **15**, 7031−7037.

Graphic abstract for:

Predicting and creating 7-connected Zn_4O vertices for the construction of exceptional metal-organic framework with nanoscale cages

Shizhe Bai, Weiquan Zhang, Yun Ling, Feilong Yang, Mingli Deng, Zhenxia Chen, Linhong Weng, and Yaming Zhou

The 7-connected Zn_4O vertices has been theoretically predicted based on the model of basic zinc acetate $[Zn_4O(CH_3COO)_6]$, which was then experimentally extended into three-dimensional structure featuring three kinds of nanocages in a unit cell.